Molecular Therapy
Oncolytics
Original Article

Ablation of Stromal Cells with a Targeted Proapoptotic Peptide Suppresses Cancer Chemotherapy Resistance and Metastasis

Fei Su,[1] Xiaoping Wang,[2,3,4] Troy Pearson,[2,3,4] Jangsoon Lee,[2,3,4] Savitri Krishnamurthy,[2,5] Naoto T. Ueno,[2] and Mikhail G. Kolonin[1]

[1]The Brown Foundation Institute of Molecular Medicine for the Prevention of Human Disease, The University of Texas Health Sciences Center at Houston, Houston, TX 77030, USA; [2]Morgan Welch Inflammatory Breast Cancer Research Program and Clinic, The University of Texas MD Anderson Cancer Center, Houston, TX, USA; [3]Section of Translational Breast Cancer Research, The University of Texas MD Anderson Cancer Center, Houston, TX, USA; [4]Department of Breast Medical Oncology, The University of Texas MD Anderson Cancer Center, Houston, TX, USA; [5]Department of Pathology, The University of Texas MD Anderson Cancer Center, Houston, TX, USA

Adipose stromal cells (ASCs) recruited by tumors contribute to the population of cancer-associated fibroblasts. ASCs have been reported to induce tumor growth and chemotherapy resistance. The effect of ASCs on metastasis has not been explored. Here, we investigated the role of ASCs in cancer aggressiveness and tested them as a therapy target. We show that ASCs promote the epithelial-mesenchymal transition and invasiveness of triple-negative breast cancer cells. In human cell lines derived from various types of breast tumors, ASCs suppressed cytotoxicity of cisplatin and paclitaxel. D-CAN, a proapoptotic peptide targeting ASC, suppressed spontaneous breast cancer lung metastases in a mouse allograft model when combined with cisplatin. Moreover, in a human breast cancer xenograft model, treatment with D-CAN alone was sufficient to suppress lung metastases. This study improves our understanding of how tumor stromal cells recruited from fat tissue stimulate carcinoma progression to chemotherapy resistance/metastasis and outlines a new approach to combination cancer treatment.

INTRODUCTION

Breast carcinomas (BCas) develop resistance to therapy and distant metastases as a result of dynamic interaction with tumor stroma, which is composed of various nonmalignant cell types.[1] Cancer-associated fibroblasts (CAFs), the mesenchymal stromal cells (MSCs) of tumors, are a population of cells in carcinomas that have stirred controversy.[2] Whereas CAFs have been reported to promote cancer progression,[3,4] attempts to inactivate them have produced conflicting results.[5,6] The underlying mechanisms of CAF effects are poorly understood.[7,8] CAFs play multiple roles, including leukocyte recruitment, extracellular matrix (ECM) remodeling, vascularization, and immunosuppression.[9] It has been proposed that CAFs mute the anti-tumor immune response through their effects on T cells and are partly responsible for the inefficacy of immunotherapy in BCas and other carcinomas.[8,10,11] A key function of CAFs appears to be their ability to induce epithelial-mesenchymal transition (EMT) of carcinoma cells.[12] Whereas the role of EMT in metastatic dissemination is debated,[13] acquisition of the "cancer stem cell" properties and resistance to chemotherapy are undoubtedly hallmarks of EMT.[7] Selective CAF-targeting therapies are lacking, and their development is highly anticipated.[14]

CAFs are derived from distinct lineages and are heterogeneous.[2,7] Recent reports provide evidence that CAFs are, at least in part, derived from white adipose tissue (WAT) surrounding the tumor.[15–17] Progression of BCas and other carcinomas is aggravated by obesity.[18,19] Our studies in mouse models have shown that WAT, which becomes inflamed and fibrotic in obesity, enhances cancer progression irrespective of diet[20] and that WAT transplantation is linked with a higher likelihood of BCa relapse.[21] Peritumoral WAT undergoing remodeling in cancer plays a particularly important role in several types of cancer. Our studies indicate that adipose stromal cells (ASCs), the MSC of WAT, are expanded in obesity, become mobilized, and migrate to tumors.[22] This process, particularly prominent in obese cancer patients, is linked with poor cancer prognosis.[22] There is accumulating evidence that ASC-infiltrating tumors from adjacent WAT depots contribute to the population of CAF-promoting cancer through a multitude of mechanisms.[20,22,23] A role for ASCs in therapy resistance has surfaced,[24] identifying these cells as a prospective drug target.[25]

By screening a combinatorial library *in vivo*, we had previously isolated a cyclic peptide WAT7 (sequence CSWKYWFGEC) that homes to ASC in both WAT and tumors.[26,27] We have modified it into a compound targeting ASC, termed D-CAN, which can be used for selective ASC depletion.[27,28] By using this reagent, we recently demonstrated the role of adipose-derived CAF in EMT induction,

Received 19 June 2020; accepted 21 August 2020;
https://doi.org/10.1016/j.omto.2020.08.012.

Correspondence: Mikhail G. Kolonin, PhD, The Brown Foundation Institute of Molecular Medicine for the Prevention of Disease, The University of Texas Health Science Center at Houston, 1825 Pressler St., 430E, Houston, TX 77030, USA.
E-mail: mikhail.g.kolonin@uth.tmc.edu

invasiveness, and chemoresistance of prostate cancer cells.[29] However, a possible role of ASC in metastatic progression has not been explored.

Here, we hypothesized that ASCs promote EMT of BCas. We demonstrate that ASC-derived factors induce EMT, invasiveness, and chemoresistance of BCa cells. Importantly, ASC depletion suppressed spontaneous metastases of mouse and human BCa tumor grafts. We conclude that ASC-derived CAFs are an important drug target, inactivation of which can synergize with chemotherapy.

RESULTS

ASCs Induce EMT and Invasiveness in BCa Cells

First, we tested if ASCs derived from mammary WAT confer EMT properties to BCa cells. In coculture with human ASCs, triple-negative mouse 4T1 cell lines transduced with mCherry were identified based on red fluorescence. 4T1 cells cultured alone displayed tight junctions typical of epithelium and expressed an epithelial marker E-cadherin, as revealed by immunofluorescence (IF). In contrast, ASC coculture resulted in a switch to mesenchymal fibroblastic morphology and E-cadherin downregulation (Figure 1A). We confirmed our findings in primary BCa cells derived from mouse mammary tumor virus (MMTV)-polyoma virus middle T (PyMT); fibroblast specific protein 1 (Fsp1)-cre; Rosa26-red fluorescent protein (RFP)-GFP mice, which undergo an irreversible switch from membrane Tomato (mT) red (RFP+GFP−) to membrane green (mG; or RFP−GFP+) fluorescence upon Fsp1 promoter activation in mesenchymal lineage.[13] A short-term coculture with human mammary ASCs resulted in the appearance of yellow RFP+GFP+ cells undergoing EMT and with mesenchymal morphology observed for GFP+ cells (Figure 1B). This result was quantified by flow cytometry, which showed that the frequency of RFP+GFP+ cells increased from 5% to 14% upon ASC coculture (Figure 1C). To confirm these results in a human cancer cell model, we used cell lines derived from patients with inflammatory BCa, an aggressive carcinoma subtype of breast cancer featuring inflammation and a high rate of metastasis.[30,31] Culture in conditioned medium (CM) from human subcutaneous ASC was sufficient to induce mesenchymal morphology in SUM149 and SUM190 cells (Figure S1A). EMT induction was confirmed by immunoblotting, demonstrating the induction of mesenchymal marker N-cadherin concomitant with increased fibronectin deposition (Figure S1B).

Because EMT is coupled with induction of cell motility, we tested if ASC coculture promotes migration of cancer cells. ASC from both mammary and subcutaneous WAT (SAT) induced Transwell migration of 4T1, SUM149, as well as MCF7 human BCa cells upon coculture (Figure 1D). Mammary ASC induced migration of MCF7 cells more efficiently, whereas the effect of SAT and mammary ASC on mouse and human triple-negative BCa cells was comparable (Figure 1E). ASC CM was sufficient to induce migration of SUM149 and KPL-4 cells in the Transwell assay (Figure S1C). ASC CM also promoted invasion of human BCa cells (Figure S1D).

ASCs Induce Chemotherapy Resistance in BCa Cells

Next, we tested if ASCs confer BCa cells' chemoresistance, a reported attribute of EMT. Upon treatment of MMTV-PyMT; Fsp1-cre; Rosa26-RFP-GFP BCa cells with a DNA crosslinker cisplatin, the frequency of RFP+GFP− cells was reduced from 56% (Figure 1C) to 39% (Figure 2A), indicating a relatively low resistance of epithelial cells. Upon ASC coculture, the majority (50%) of cisplatin-surviving cells were GFP+RFP− (50%) and GFP+RFP+ (9%), compared to 38% and 14.2%, respectively, in the nontreatment group (Figure 2A). The ratio of (GFP+RFP− + GFP+RFP+)/GFP−RFP+ for cisplatin-treated ASC coculture was significantly higher: 1.6, compared to 0.82 for the no-treatment group (Figure 2B).

We also preformed experiments with human cancer cells transduced with GFP, which were quantified based on fluorescence in ASC coculture. MCF7 and SUM149 cells displayed increased resistance to cisplatin and microtubule disruptor paclitaxel when cocultured with mammary or subcutaneous ASCs (Figure 2C). Cell death upon treatment with these chemotherapeutics was quantified based on propidium iodide uptake (Figure 2D). MCF7 and SUM149 cell death in response to cisplatin and paclitaxel was significantly reduced by ASC coculture (Figure 2E). Combined, these data indicate that ASCs induce an aggressive phenotype in carcinoma cells via EMT promotion.

ASC Depletion/Chemotherapy Combination Suppresses Metastases of 4T1 Allografts

We investigated the effect of ASC depletion on breast tumor aggressiveness at advanced cancer stages by using the previously validated ASC-targeting peptide D-CAN.[26–29] BALB/c mice, orthotopically grafted with 4T1 cells expressing luciferase into a mammary fat pad for noninvasive tumor tracking, were treated with cisplatin (0.6 or 3.0 mg/kg), D-CAN (0.75 mg/kg), or a combination of 0.6 mg/kg cisplatin and D-CAN from the day tumors became palpable. Compared with saline (PBS) sham-injected controls, a cisplatin dose of 0.6 mg/kg had only a subtle effect on tumor growth (Figure 3A). D-CAN also did not have a significant effect on tumor growth (Figure 3A). A cisplatin dose of 3.0 mg/kg suppressed tumor growth (Figure 3A); however, mice have become moribund, and lethality was observed after day 10 of treatment (Figures 3A and 3B). Tumors in mice treated with a 0.6-mg/kg cisplatin + D-CAN combination were significantly smaller at the terminal time point than in mice treated with individual agents (Figure 3A). Importantly, in the combination group, no signs of toxicity were observed, and all mice have survived to the time point at which the majority of mice in the other groups have died (Figure 3B). Individual tumor analysis upon necropsy confirmed a significantly smaller endpoint tumor weight (Figures S2A and S2B) in the "cisplatin + D-CAN" group compared to the "cisplatin-only" control. Tumors in the cisplatin + D-CAN group displayed wider areas of necrosis, compared to low-dose cisplatin-only and "D-CAN-only" groups (Figure S2C). Whereas in the cisplatin-only group, viable tumor areas had prominent fibronectin deposition and a low frequency of cells expressing

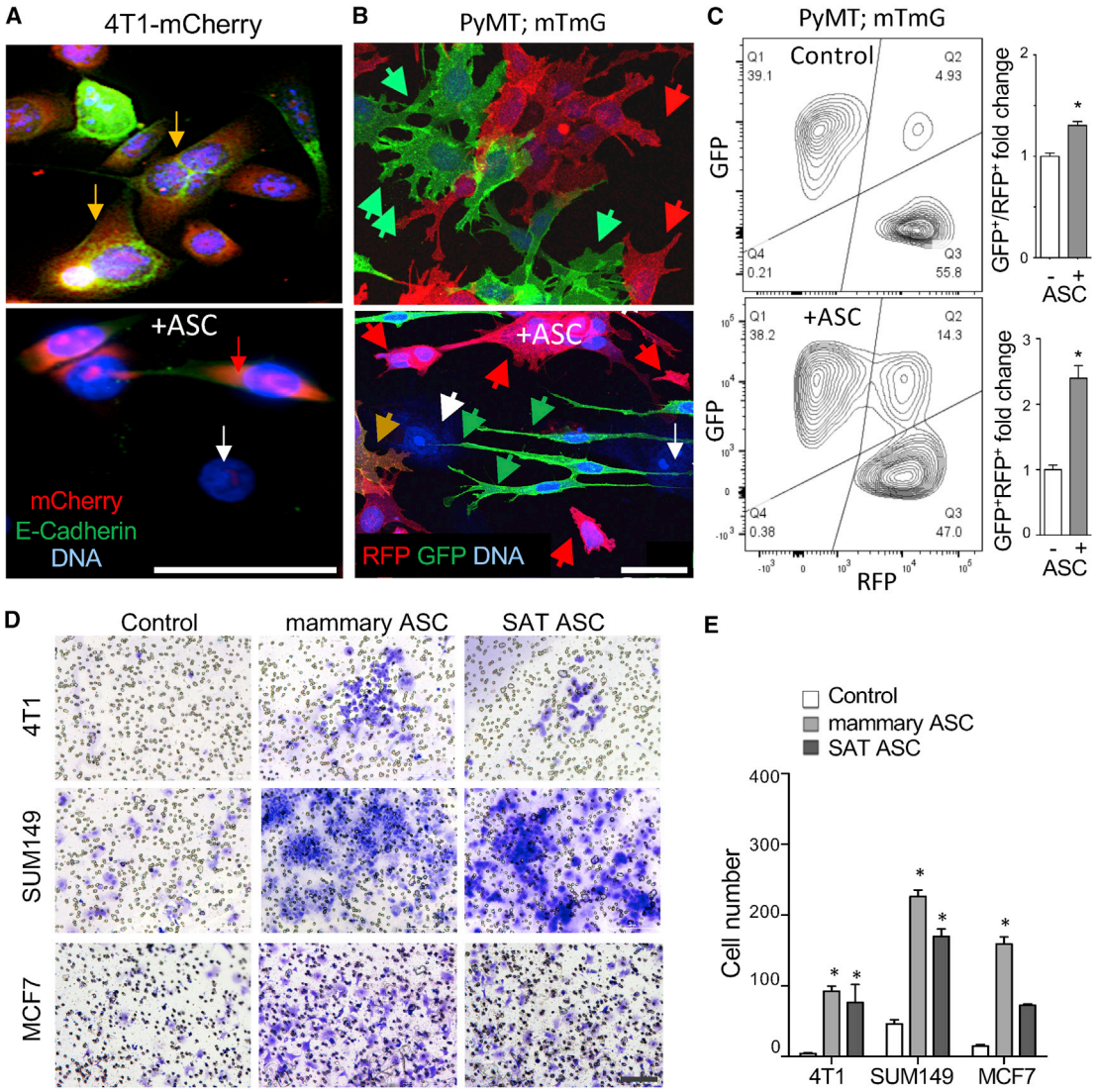

Figure 1. ASCs Induce EMT and Invasiveness in Breast Carcinoma

(A) Coculture with mammary ASCs induces mesenchymal morphology in RFP-labeled BCa 4T1 cells (red). Tight junction E-cadherin detected by IF (green) in epithelial cells (yellow) is lost upon EMT. White arrow, ASCs detected by nuclear staining (blue). (B) EMT detected by lineage tracing in BCa cells from *MMTV-PyMT; Fsp1-cre; Rosa26-RFP-GFP* mice cocultured with human mammary ASC. Note induced RFP+GFP+ cells (yellow) and mesenchymal morphology of GFP+ cells (green). (C) Flow cytometry on cells from (B) GFP+ cells demonstrates GFP induction by ASC coculture, quantified on the right for total GFP+ and GFP+RFP+ cells. (D) 4T1, SUM149, and MCF7 cells migrated across the Transwell membrane stained with crystal violet after 48 h of coculture with ASC from human mammary WAT or subcutaneous WAT (SAT). (E) Quantification of ASC effect on migrated cancer cell number in experiment (D). Shown are mean ± SEM of N = 10 view fields. For all data, *p < 0.05, unpaired Student's t test. Scale bars, 50 μm. See also Figure S1.

E-cadherin, these hallmarks of EMT were suppressed in the cisplatin + D-CAN combination group (Figure S2D).

To determine the effect of ASC on metastasis, we analyzed lungs, the main site of spontaneous BCa dissemination in mouse models. Reduced recovery of metastatic cells from the lung, as measured by thioguanine selection of lung-derived cells in culture,[32] was observed after a high dose (15 mg/kg) of D-CAN treatment alone (Figure S2E). However, this could due to a direct inhibitory D-CAN effect on the primary tumor observed at that dose.[27] Therefore, we analyzed the D-CAN combination effects at the dose that does not reduce primary tumor growth. The use of 4T1 cells expressing luciferase enabled noninvasive *In Vivo* Imaging System (IVIS) visualization of lung metastases, which were observed for the control, "cisplatin-alone," and "D-CAN-alone" groups; in contrast, no lung metastases were observed in the 'cisplatin + D-CAN' combination group (Figure S2G). Upon necropsy, visual lung inspection revealed multiple macrometastases in the control and individual agent-treated groups (Figure 3C). Consistent with IVIS data,

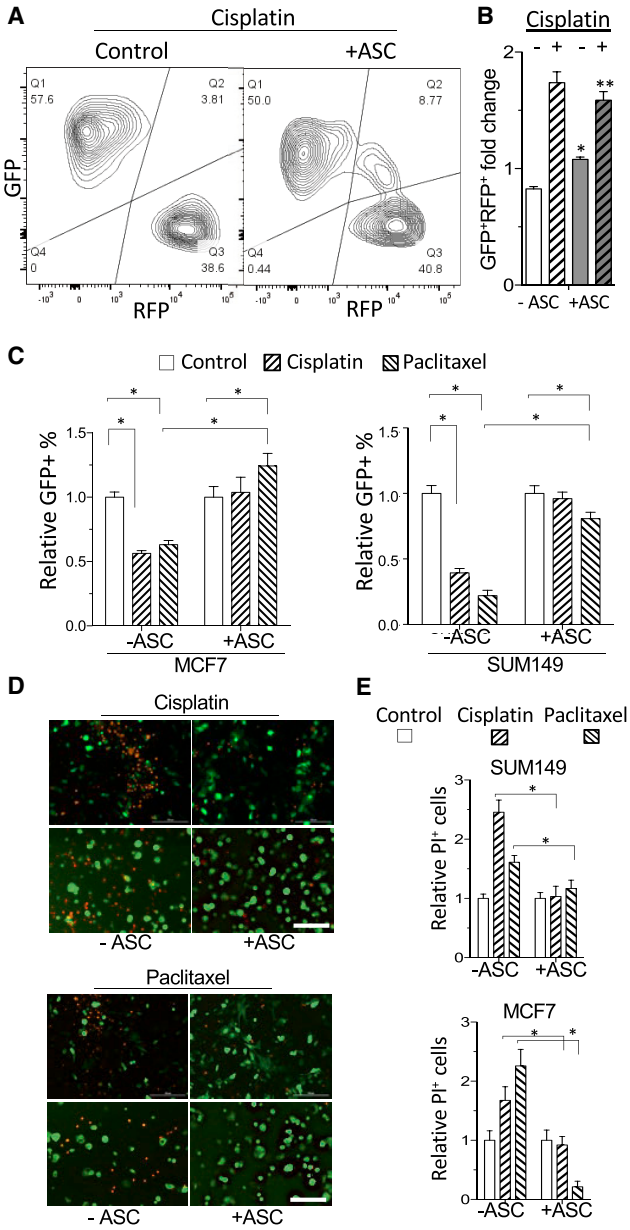

Figure 2. ASCs Induce Chemoresistance in Breast Carcinoma

(A) Flow cytometry on cisplatin-treated cells from *MMTV-PyMT; Fsp1-cre; Rosa26-RFP-GFP* mice demonstrates preferential survival of GFP+ cells compared to untreated controls (Figure 1C). (B) Flow cytometry data from (A) quantified for GFP+RFP+ cells. (C) Quantification of GFP+ MCF7 and SUM149 cells, cultured with or without (Control) human ASC, that survived cisplatin or paclitaxel treatment; normalized to no treatment (Control). Shown are mean ± SEM of N = 10 view fields. D-E, GFP+ SUM149 and MCF7 cells cultured with or without (Control) human mammary ASC were treated with cisplatin or paclitaxel. (D) Dying cells identified based on propidium iodide (PI) staining. (E) Quantified PI+ cells normalized to no treatment controls (–). For all data, shown are mean ± SEM of N = 10 view fields. *p < 0.05, unpaired Student's t test. Scale bars, 50 μm.

metastases were, with rare exception, absent in lungs of mice from the cisplatin + D-CAN group (Figure 3C), which was confirmed by mCherry fluorescence (Figure S2F). Histological examination of hematoxylin and eosin (H&E)-stained sections showed that whereas in the 0.6-mg/kg cisplatin group, metastases were abundant and large, their size tended to be smaller in the D-CAN group (Figures 3D and 3E). Importantly, histopathological quantification revealed that lung metastases were more rare in the cisplatin + D-CAN group compared to the cisplatin-alone group (Figures 3D and 3E).

ASC Depletion Suppresses Metastases of Human BCa Xenografts

To confirm these results in a human cancer model, we used orthotopic SUM149 xenografts in the mammary fat pad of immunodeficient (non-obese diabetic severe combined immunodeficiency gamma [NSG]) mice. As above, D-CAN, either alone or in combination with paclitaxel, induced marked necrosis in primary tumors (Figure 4A). Depletion of tumor stroma by D-CAN was evident from reduced deposition of C-X-C motif chemokine 12 (CXCL12), a cytokine secreted by stromal cells,[33] concomitantly with EMT suppression measured based on N-cadherin expression (Figure 4B). Metastatic dissemination, induced by surgical resection of the primary tumors as previously described,[30] was subsequently analyzed histologically in lung sections (Figure 4C) by a certified pathologist. In this model, lung metastases, which were abundant in the control group, were rare in both paclitaxel-treated and D-CAN-treated mice (Figure 4D). Importantly, whereas relatively large metastases were observed for the control and paclitaxel groups, only small micrometastases were observed for D-CAN and the combination treatment groups (Figures 4C and 4D). Together, our results demonstrate that tumor EMT can be blocked by pharmacological ASC depletion, which results in enhanced efficacy of chemotherapy and suppressed metastatic dissemination (Figure 4E).

DISCUSSION

There is an urgent need for new strategies to effectively intervene resistance of breast cancer to treatment and progression to the metastatic stage. It has been reported that CAFs promote cancer progression to metastasis.[3,34] WAT has been identified as a source of CAF.[20,22,23] In a recent study, ASC depletion enhanced chemotherapy efficacy in animal models of prostate cancer.[29] However, it has not been clear if this extends to other cancer types, and the role of ASC-derived CAF in metastatic dissemination has not been explored. Here, we investigated the role of ASC in BCa aggressiveness. With the use of breast cancer models, we show that ASCs promote EMT, migration, and chemotherapy resistance. We demonstrate that ASC depletion suppresses spontaneous BCa metastasis in xenograft models.

Clinical significance of tumor stroma derived from WAT remains to be further established. Obese patients are at a higher risk of progression to chemotherapy/immunotherapy resistance and incurable metastases.[18] The molecular signals through which adipose-derived CAFs promote cancer progression are unclear. Some of the cancer-promoting effects of ASC are contact dependent.[35] ASCs are a major source of the ECM that drives tumor desmoplasia,[36] and they also

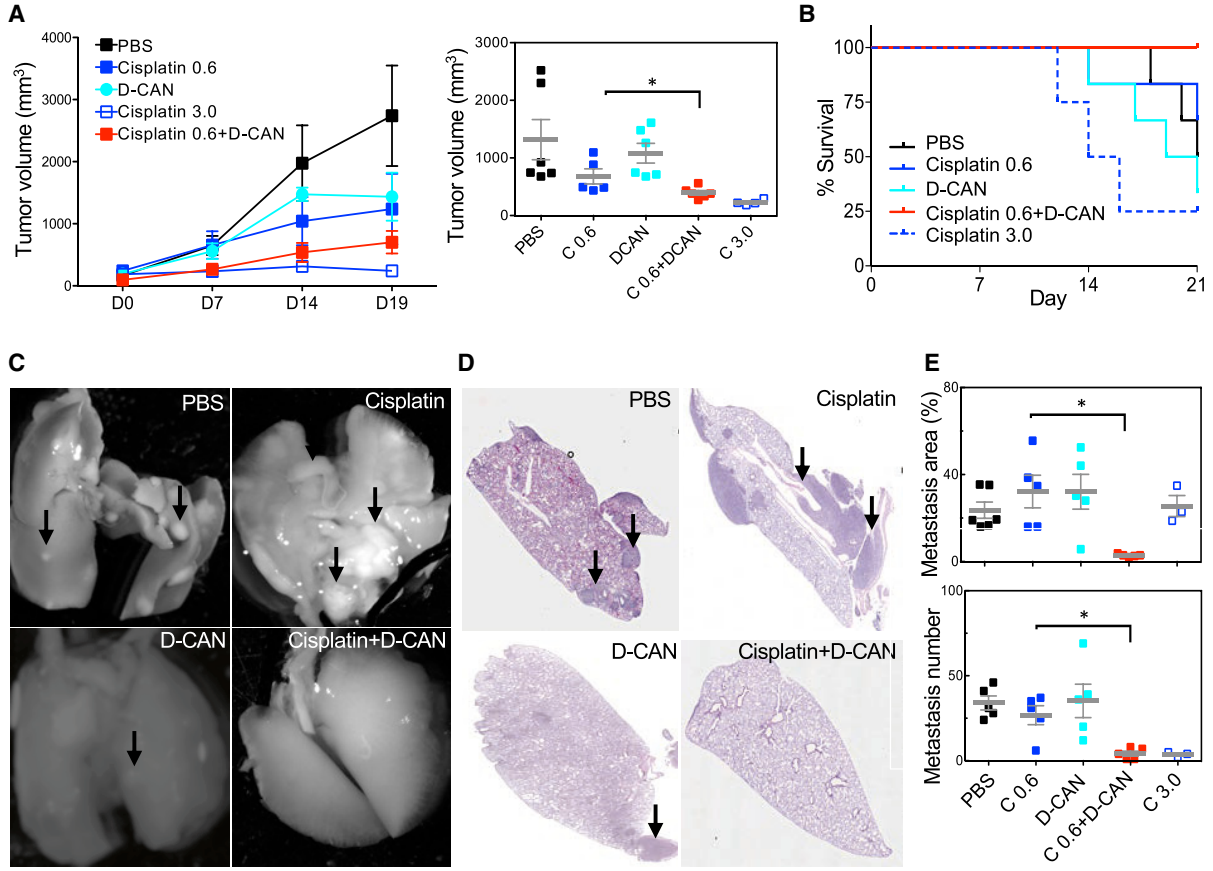

Figure 3. ASC Depletion Synergizes with Cisplatin in a Breast Cancer Metastasis Model

(A) Orthotopic 4T1 tumor growth in BALB/C mice injected with PBS, 0.75 mg/kg D-CAN, 0.6 mg/kg cisplatin (C 0.6), 3 mg/kg cisplatin (C 3.0), or 0.75 mg/kg D-CAN + 0.6 mg/kg cisplatin (N = 5 to 6/group). Injections (3/week) started when tumors reached 0.1 cm (day 1). (Right plot) Final tumor volume; *$p < 0.05$ (unpaired Student's t test) for the C 0.6 versus C 0.6 + D-CAN group. (B) Kaplan-Meier curves showing percent survival of mice from (A). (C) Representative images of lungs from mice in (A) resected on day 20. Arrows, metastases. (D) H&E stainings of lungs from mice in (A) resected on day 20 post-tumor grafting. (E) Metastatic area determined with NIH ImageJ software by analysis of 10× fields and mean number of metastases/lung quantified through analysis of sections in (D). *$p < 0.05$ (unpaired Student's t test). Scale bar, 250 μm. See also Figure S2.

secrete trophic factors that stimulate vascularization.[20,23] ASC-derived factors inducing the EMT remain to be identified. Insights into the mechanisms underlying the link between tumor aggressiveness and fat tissue may enable new approaches to disease intervention. Further studies will be needed to evaluate WAT-derived CAF as a modulator of immune cell activation in the tumor and a prospective therapy target. Development of compounds targeting CAFs or blocking their activity may improve outcomes for patients with disease resistant to chemotherapy and immunotherapy. Specifically, the ASC ablation strategy may have important implications for patients with metastatic carcinoma. Clinical trials with cell-targeting peptides analogous to the one used in this study[37] pave the way to the future translation of D-CAN or its derivatives.

Conclusions

Our study improves our understanding of how tumor stroma stimulates carcinoma progression to chemotherapy resistance and metastasis. By discovering that ASCs promote the EMT and testing an ASC-targeting compound in spontaneous metastasis models, we outline a new approach to aggressive breast cancer intervention.

MATERIALS AND METHODS

Cell Culture

SAT ASCs were from bariatric surgery patients described previously.[26] Mammary ASCs (subcutaneous breast preadipocytes BR-F) were purchased from ZenBio. Cell lines 4T1, SUM149, SUM190, and KPL-4 have been used as in our previous studies.[27] MCF7 cells were purchased from ATCC. RFP+/GFP+ mixture of tumor-derived cells from *MMTV-PyMT; Fsp1-cre; Rosa26-RFP-GFP* mice described previously[13] were received from Weill Cornell. ASCs were grown in EBM (endothelial cell growth basal medium)-2 (Lonza). For coculture experiments, Ham's F-12 medium was used for SUM149 cells, and DMEM was used for MCF7 cells.

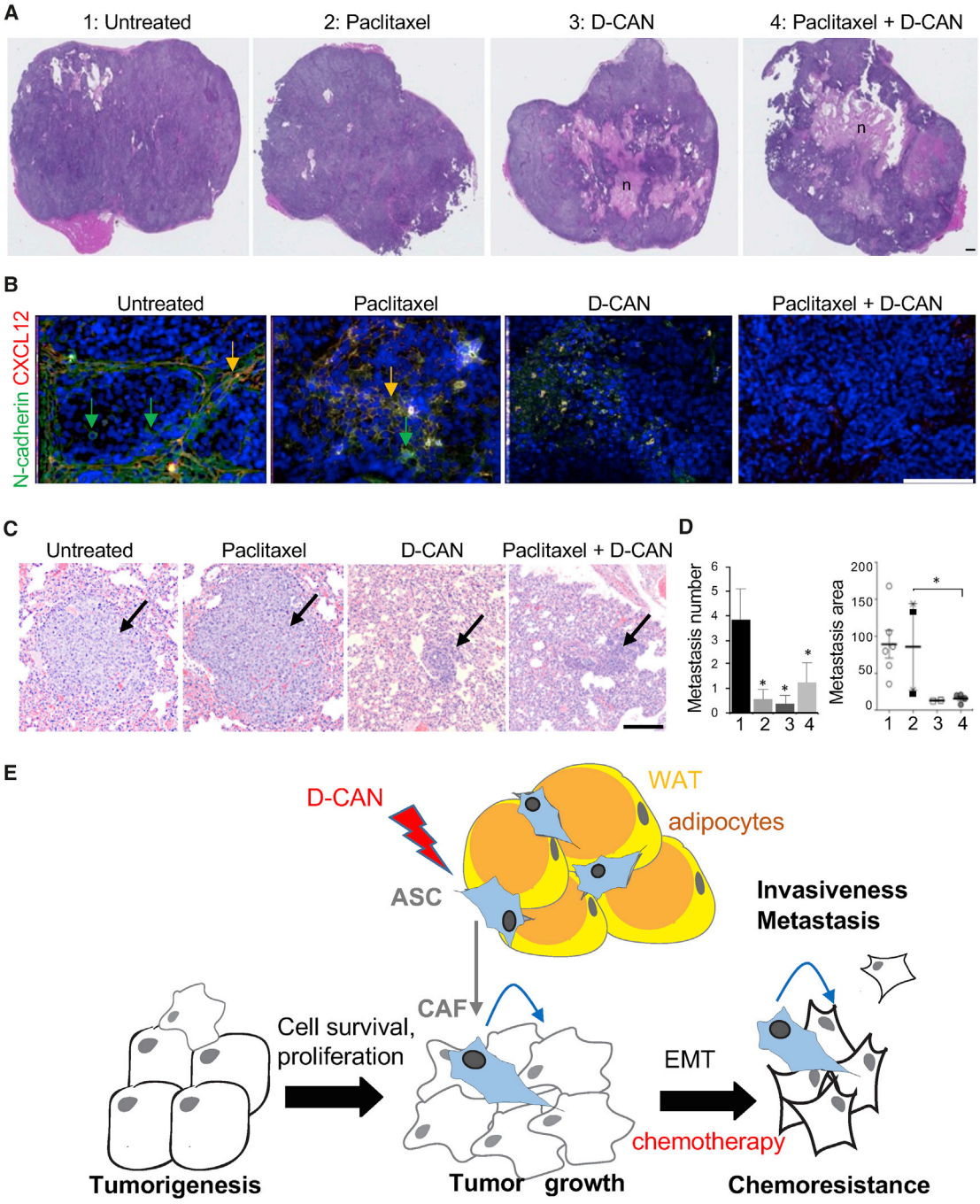

Figure 4. ASC Depletion Suppresses Metastases in a Breast Cancer Xenograft Model

(A) H&E stainings of orthotopic SUM149 tumors grown in NSG mice injected with (1) PBS; (2) paclitaxel (7.5 mg/kg, intravenously [i.v.], 1/week); (3) D-CAN (1.1 mg/kg, subcutaneously [s.c.], 2/week); or (4) D-CAN + paclitaxel combination (N = 10/group). n, necrosis. (B) IF on tumor sections from mice in (A) showing reduction in CXCL12+ stromal cells and of N-cadherin+ cancer cells in tumors of mice treated with D-CAN. Nuclei are blue. (C) Micrographs of H&E-stained lung areas containing the largest metastases observed in mice from (A). (D) Quantification of metastases in mice from (C). Number: per lung; area: ImageJ pixels. Shown are mean ± SEM. *$p < 0.05$ (unpaired Student's t test). Scale bars, 250 μm. (E) The model of the ASC role in cancer progression. ASCs derived from WAT and becoming CAFs initially increase the survival and proliferation of cancer cells and subsequently their EMT, chemotherapy resistance, invasiveness, and metastatic dissemination. Lightning bolt, D-CAN as an experimental therapeutic that can be used to deplete ASCs and suppress cancer progression.

ASCs were seeded first in a 96-well plate (0.5×10^3/well); after they adhered, cancer cells were seeded on top (3×10^3/well). For flow cytometry, RFP+/GFP+ cells detached with trypsin were pregated to exclude debris, cell clumps, as well as dead cells based on 4′,6-diamidino-2-phenylindole (DAPI) staining, and then 10,000 live singlets were gated and quantified based on RFP fluorescence and GFP fluorescence with FACSAria/FlowJo software (BD Biosciences) as described.[20] Cisplatin (VWR; 95031-032) was used at 5 μg/mL. Paclitaxel (Selleckchem; S1150) was used at 5 ng/mL. Cancer cell numbers in coculture were determined using Cytation5 (Biotek)/Gen5 software by total nucleated GFP+ cell counts as described.[29] Transwell assays were performed as described:[22,33] cancer cells were seeded onto the upper chamber of a Transwell filter with 8 μm pores (Costar) after serum starvation for 4 h. Nonmigrated cells on top of filters were removed using a cotton-tipped swab, and migrated cells at the bottom of the filter were fixed and stained with 0.4% crystal violet in 10% ethanol.

Mouse Experiments

Studies were approved by and performed according to the guidelines of the Institutional Animal Care and Use Committees of UTHealth and MD Anderson Cancer Center. BALB/C mice were purchased from Jackson Laboratory. NSG mice were purchased from Envigo. Orthotopic grafting of 4T1 cells into the mammary fat pad was performed as previously described.[27,30] For SUM149 mammary fat pad grafting, 4×10^6 cells in 50% Matrigel were injected. Drug treatment began when tumors became detectable. D-CAN, composed of ASC-homing peptide WAT7 (CSWKYWFGEC), linked via aminohexanoic acid with an amphipathic sequence KFAKFAKKFAKFAK,[27] was synthesized from D-amino acids and cysteine cyclized and acetate salt chromatographically purified to 99% and quality controlled (mass spectroscopy) by Ambiopharm. D-CAN was injected subcutaneously as described.[27,29] Cisplatin and paclitaxel were administered intravenously. Tumors were harvested and processed when they exceeded 1.5 cm^3 or became ulcerated in the PBS-injected group. Primary SUM149 tumors at approximately 500 mm^3 were surgically removed after treatment for 20 days, and mice were treated for 6 more weeks, after which, lungs were collected for metastasis analysis. Tumor size was measured with a caliper; volume was calculated as length $\times$ width^2 $\times$ 0.52. Xenogen IVIS imaging was performed as described.[30]

IF

Tissues were fixed in 10% formalin, paraffin embedded, and sectioned for IF and H&E staining. Cultured cells were fixed in 4% paraformaldehyde. For IF, performed as described,[22,29,33] primary antibodies were as follows: anti-E-cadherin R&D AF748 (1:100); anti-N-cadherin ab98952 (Abcam; 1:100); anti-CXCL12 sc-28876 (1:200); anti-fibronectin ab23750 (1:200); anti-GFP GTX26673; 1:250 (1:200). Secondary antibodies were donkey Alexa 488-conjugated immunoglobulin G (IgG) or cyanine (Cy)3-conjugated IgG (Jackson ImmunoResearch; 1:300). Nuclei were stained with DAPI. Images were acquired with Carl Zeiss Apotome Axio Imager Z1.

Statistics

GraphPad Prism or Microsoft Excel was used to graph data as mean ± SEM and to calculate p values using the homoscedastic Student's t test for most experiments, which were repeated at least twice with similar results. For metastasis quantification, ANOVA and Tukey-Kramer multiple comparison tests and Kruskal-Wallis and Dunn's post-test with Sidak correction were used to examine the differences between study arms.

SUPPLEMENTAL INFORMATION

Supplemental Information can be found online at https://doi.org/10.1016/j.omto.2020.08.012.

AUTHOR CONTRIBUTIONS

Conceptualization, M.G.K., F.S., and N.T.U.; Investigation, F.S., X.W., T.P., J.L., and S.K.; Writing – Review & Editing, M.G.K., F.S., and N.T.U.; Administration, M.G.K. and N.T.U.; Supervision, M.G.K. and N.T.U.

CONFLICTS OF INTEREST

The authors declare no competing interests.

ACKNOWLEDGMENTS

We thank Dingcheng Gao for *MMTV-PyMT*; *Fsp1-cre*; *Rosa26-RFP-GFP* cells and Sendurai Mani for luciferase-expressing 4T1 cells. We thank Alexes Daquinag, Wanqiao Cao, and Zhengmei Mao for technical help. This study was funded by grant 1R21 CA216745-01A1 from the National Institutes of Health and by the Harry E. Bovay, Jr. Foundation.

REFERENCES

1. Hanahan, D., and Coussens, L.M. (2012). Accessories to the crime: functions of cells recruited to the tumor microenvironment. Cancer Cell *21*, 309–322.
2. Sahai, E., Astsaturov, I., Cukierman, E., DeNardo, D.G., Egeblad, M., Evans, R.M., Fearon, D., Greten, F.R., Hingorani, S.R., Hunter, T., et al. (2020). A framework for advancing our understanding of cancer-associated fibroblasts. Nat. Rev. Cancer *20*, 174–186.
3. Karnoub, A.E., Dash, A.B., Vo, A.P., Sullivan, A., Brooks, M.W., Bell, G.W., Richardson, A.L., Polyak, K., Tubo, R., and Weinberg, R.A. (2007). Mesenchymal stem cells within tumour stroma promote breast cancer metastasis. Nature *449*, 557–563.
4. Bhowmick, N.A., Neilson, E.G., and Moses, H.L. (2004). Stromal fibroblasts in cancer initiation and progression. Nature *432*, 332–337.
5. Olive, K.P., Jacobetz, M.A., Davidson, C.J., Gopinathan, A., McIntyre, D., Honess, D., Madhu, B., Goldgraben, M.A., Caldwell, M.E., Allard, D., et al. (2009). Inhibition of Hedgehog signaling enhances delivery of chemotherapy in a mouse model of pancreatic cancer. Science *324*, 1457–1461.
6. Özdemir, B.C., Pentcheva-Hoang, T., Carstens, J.L., Zheng, X., Wu, C.C., Simpson, T.R., Laklai, H., Sugimoto, H., Kahlert, C., Novitskiy, S.V., et al. (2015). Depletion of Carcinoma-Associated Fibroblasts and Fibrosis Induces Immunosuppression and Accelerates Pancreas Cancer with Reduced Survival. Cancer Cell *28*, 831–833.
7. LeBleu, V.S., and Kalluri, R. (2018). A peek into cancer-associated fibroblasts: origins, functions and translational impact. Dis. Model. Mech. *11*, dmm029447.
8. Ziani, L., Chouaib, S., and Thiery, J. (2018). Alteration of the Antitumor Immune Response by Cancer-Associated Fibroblasts. Front. Immunol. *9*, 414.
9. Gascard, P., and Tlsty, T.D. (2016). Carcinoma-associated fibroblasts: orchestrating the composition of malignancy. Genes Dev. *30*, 1002–1019.

10. Feig, C., Jones, J.O., Kraman, M., Wells, R.J., Deonarine, A., Chan, D.S., Connell, C.M., Roberts, E.W., Zhao, Q., Caballero, O.L., et al. (2013). Targeting CXCL12 from FAP-expressing carcinoma-associated fibroblasts synergizes with anti-PD-L1 immunotherapy in pancreatic cancer. Proc. Natl. Acad. Sci. USA *110*, 20212–20217.
11. Chen, I.X., Chauhan, V.P., Posada, J., Ng, M.R., Wu, M.W., Adstamongkonkul, P., Huang, P., Lindeman, N., Langer, R., and Jain, R.K. (2019). Blocking CXCR4 alleviates desmoplasia, increases T-lymphocyte infiltration, and improves immunotherapy in metastatic breast cancer. Proc. Natl. Acad. Sci. USA *116*, 4558–4566.
12. Orimo, A., and Weinberg, R.A. (2006). Stromal fibroblasts in cancer: a novel tumor-promoting cell type. Cell Cycle *5*, 1597–1601.
13. Fischer, K.R., Durrans, A., Lee, S., Sheng, J., Li, F., Wong, S.T., Choi, H., El Rayes, T., Ryu, S., Troeger, J., et al. (2015). Epithelial-to-mesenchymal transition is not required for lung metastasis but contributes to chemoresistance. Nature *527*, 472–476.
14. Chen, X., and Song, E. (2019). Turning foes to friends: targeting cancer-associated fibroblasts. Nat. Rev. Drug Discov. *18*, 99–115.
15. Laurent, V., Toulet, A., Attané, C., Milhas, D., Dauvillier, S., Zaidi, F., Clement, E., Cinato, M., Le Gonidec, S., Guérard, A., et al. (2019). Periprostatic Adipose Tissue Favors Prostate Cancer Cell Invasion in an Obesity-Dependent Manner: Role of Oxidative Stress. Mol. Cancer Res. *17*, 821–835.
16. Bochet, L., Lehuédé, C., Dauvillier, S., Wang, Y.Y., Dirat, B., Laurent, V., Dray, C., Guiet, R., Maridonneau-Parini, I., Le Gonidec, S., et al. (2013). Adipocyte-derived fibroblasts promote tumor progression and contribute to the desmoplastic reaction in breast cancer. Cancer Res. *73*, 5657–5668.
17. Kolonin, M.G., and DiGiovanni, J. (2019). The role of adipose stroma in prostate cancer aggressiveness. Transl. Androl. Urol. *8* (*Suppl 3*), S348–S350.
18. Lengyel, E., Makowski, L., DiGiovanni, J., and Kolonin, M.G. (2018). Cancer as a Matter of Fat: The Crosstalk between Adipose Tissue and Tumors. Trends Cancer *4*, 374–384.
19. Lauby-Secretan, B., Scoccianti, C., Loomis, D., Grosse, Y., Bianchini, F., and Straif, K.; International Agency for Research on Cancer Handbook Working Group (2016). Body Fatness and Cancer–Viewpoint of the IARC Working Group. N. Engl. J. Med. *375*, 794–798.
20. Zhang, Y., Daquinag, A.C., Amaya-Manzanares, F., Sirin, O., Tseng, C., and Kolonin, M.G. (2012). Stromal progenitor cells from endogenous adipose tissue contribute to pericytes and adipocytes that populate the tumor microenvironment. Cancer Res. *72*, 5198–5208.
21. Bertolini, F., Petit, J.Y., and Kolonin, M.G. (2015). Stem cells from adipose tissue and breast cancer: hype, risks and hope. Br. J. Cancer *112*, 419–423.
22. Zhang, T., Tseng, C., Zhang, Y., Sirin, O., Corn, P.G., Li-Ning-Tapia, E.M., Troncoso, P., Davis, J., Pettaway, C., Ward, J., et al. (2016). CXCL1 mediates obesity-associated adipose stromal cell trafficking and function in the tumour microenvironment. Nat. Commun. *7*, 11674–11690.
23. Zhang, Y., Daquinag, A., Traktuev, D.O., Amaya-Manzanares, F., Simmons, P.J., March, K.L., Pasqualini, R., Arap, W., and Kolonin, M.G. (2009). White adipose tissue cells are recruited by experimental tumors and promote cancer progression in mouse models. Cancer Res. *69*, 5259–5266.
24. Nowicka, A., Marini, F.C., Solley, T.N., Elizondo, P.B., Zhang, Y., Sharp, H.J., Broaddus, R., Kolonin, M., Mok, S.C., Thompson, M.S., et al. (2013). Human omental-derived adipose stem cells increase ovarian cancer proliferation, migration, and chemoresistance. PLoS ONE *8*, e81859.
25. Rowan, B.G., Gimble, J.M., Sheng, M., Anbalagan, M., Jones, R.K., Frazier, T.P., Asher, M., Lacayo, E.A., Friedlander, P.L., Kutner, R., and Chiu, E.S. (2014). Human adipose tissue-derived stromal/stem cells promote migration and early metastasis of triple negative breast cancer xenografts. PLoS ONE *9*, e89595.
26. Daquinag, A.C., Dadbin, A., Snyder, B., Wang, X., Sahin, A.A., Ueno, N.T., and Kolonin, M.G. (2017). Non-glycanated Decorin Is a Drug Target on Human Adipose Stromal Cells. Mol. Ther. Oncolytics *6*, 1–9.
27. Daquinag, A.C., Tseng, C., Zhang, Y., Amaya-Manzanares, F., Florez, F., Dadbin, A., Zhang, T., and Kolonin, M.G. (2016). Targeted Pro-apoptotic Peptides Depleting Adipose Stromal Cells Inhibit Tumor Growth. Mol. Ther. *1*, 34–40.
28. Daquinag, A.C., Tseng, C., Salameh, A., Zhang, Y., Amaya-Manzanares, F., Dadbin, A., Florez, F., Xu, Y., Tong, Q., and Kolonin, M.G. (2015). Depletion of white adipocyte progenitors induces beige adipocyte differentiation and suppresses obesity development. Cell Death Differ. *22*, 351–363.
29. Su, F., Ahn, S., Saha, A., DiGiovanni, J., and Kolonin, M.G. (2019). Adipose stromal cell targeting suppresses prostate cancer epithelial-mesenchymal transition and chemoresistance. Oncogene *38*, 1979–1988.
30. Zhang, D., LaFortune, T.A., Krishnamurthy, S., Esteva, F.J., Cristofanilli, M., Liu, P., Lucci, A., Singh, B., Hung, M.C., Hortobagyi, G.N., and Ueno, N.T. (2009). Epidermal growth factor receptor tyrosine kinase inhibitor reverses mesenchymal to epithelial phenotype and inhibits metastasis in inflammatory breast cancer. Clin. Cancer Res. *15*, 6639–6648.
31. Lim, B., Woodward, W.A., Wang, X., Reuben, J.M., and Ueno, N.T. (2018). Inflammatory breast cancer biology: the tumour microenvironment is key. Nat. Rev. Cancer *18*, 485–499.
32. DuPré, S.A., Redelman, D., and Hunter, K.W., Jr. (2007). The mouse mammary carcinoma 4T1: characterization of the cellular landscape of primary tumours and metastatic tumour foci. Int. J. Exp. Pathol. *88*, 351–360.
33. Saha, A., Ahn, S., Blando, J., Su, F., Kolonin, M.G., and DiGiovanni, J. (2017). Proinflammatory CXCL12-CXCR4/CXCR7 signaling axis drives Myc-induced prostate cancer in obese mice. Cancer Res. *77*, 5158–5168.
34. Jung, Y., Kim, J.K., Shiozawa, Y., Wang, J., Mishra, A., Joseph, J., Berry, J.E., McGee, S., Lee, E., Sun, H., et al. (2013). Recruitment of mesenchymal stem cells into prostate tumours promotes metastasis. Nat. Commun. *4*, 1795.
35. Chen, D., Liu, S., Ma, H., Liang, X., Ma, H., Yan, X., Yang, B., Wei, J., and Liu, X. (2015). Paracrine factors from adipose-mesenchymal stem cells enhance metastatic capacity through Wnt signaling pathway in a colon cancer cell co-culture model. Cancer Cell Int. *15*, 42–47.
36. Seo, B.R., Bhardwaj, P., Choi, S., Gonzalez, J., Andresen Eguiluz, R.C., Wang, K., Mohanan, S., Morris, P.G., Du, B., Zhou, X.K., et al. (2015). Obesity-dependent changes in interstitial ECM mechanics promote breast tumorigenesis. Sci. Transl. Med. *7*, 301ra130.
37. Pasqualini, R., Millikan, R.E., Christianson, D.R., Cardó-Vila, M., Driessen, W.H., Giordano, R.J., Hajitou, A., Hoang, A.G., Wen, S., Barnhart, K.F., et al. (2015). Targeting the interleukin-11 receptor α in metastatic prostate cancer: A first-in-man study. Cancer *121*, 2411–2421.

OMTO, Volume *18*

Supplemental Information

Ablation of Stromal Cells with a Targeted Proapoptotic Peptide Suppresses Cancer Chemotherapy Resistance and Metastasis

Fei Su, Xiaoping Wang, Troy Pearson, Jangsoon Lee, Savitri Krishnamurthy, Naoto T. Ueno, and Mikhail G. Kolonin

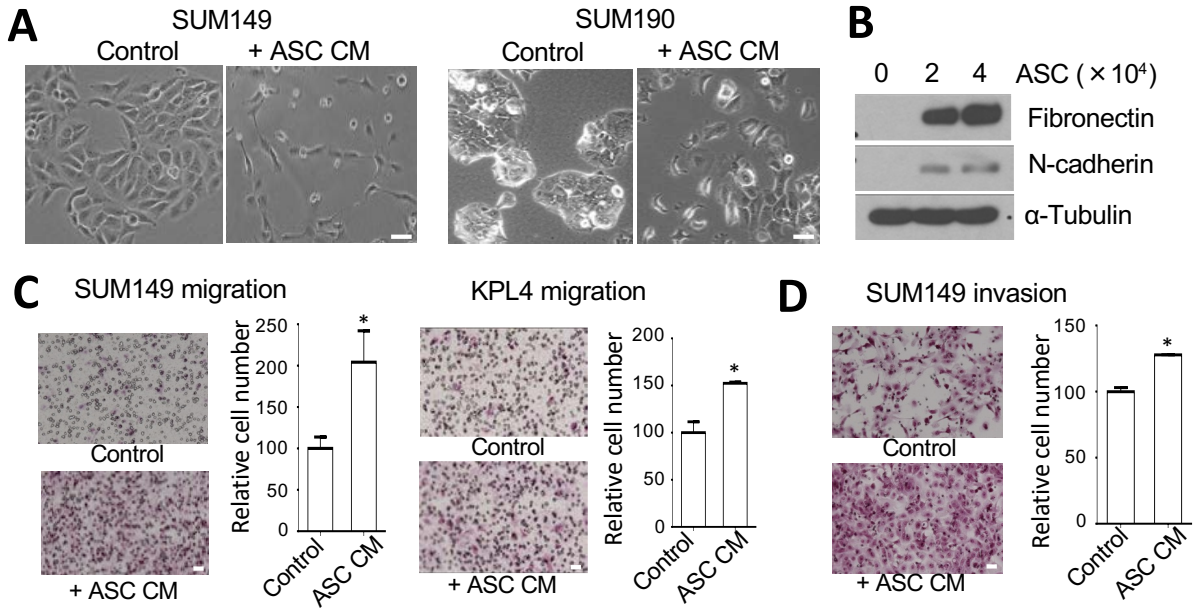

Supplementary Figure S1

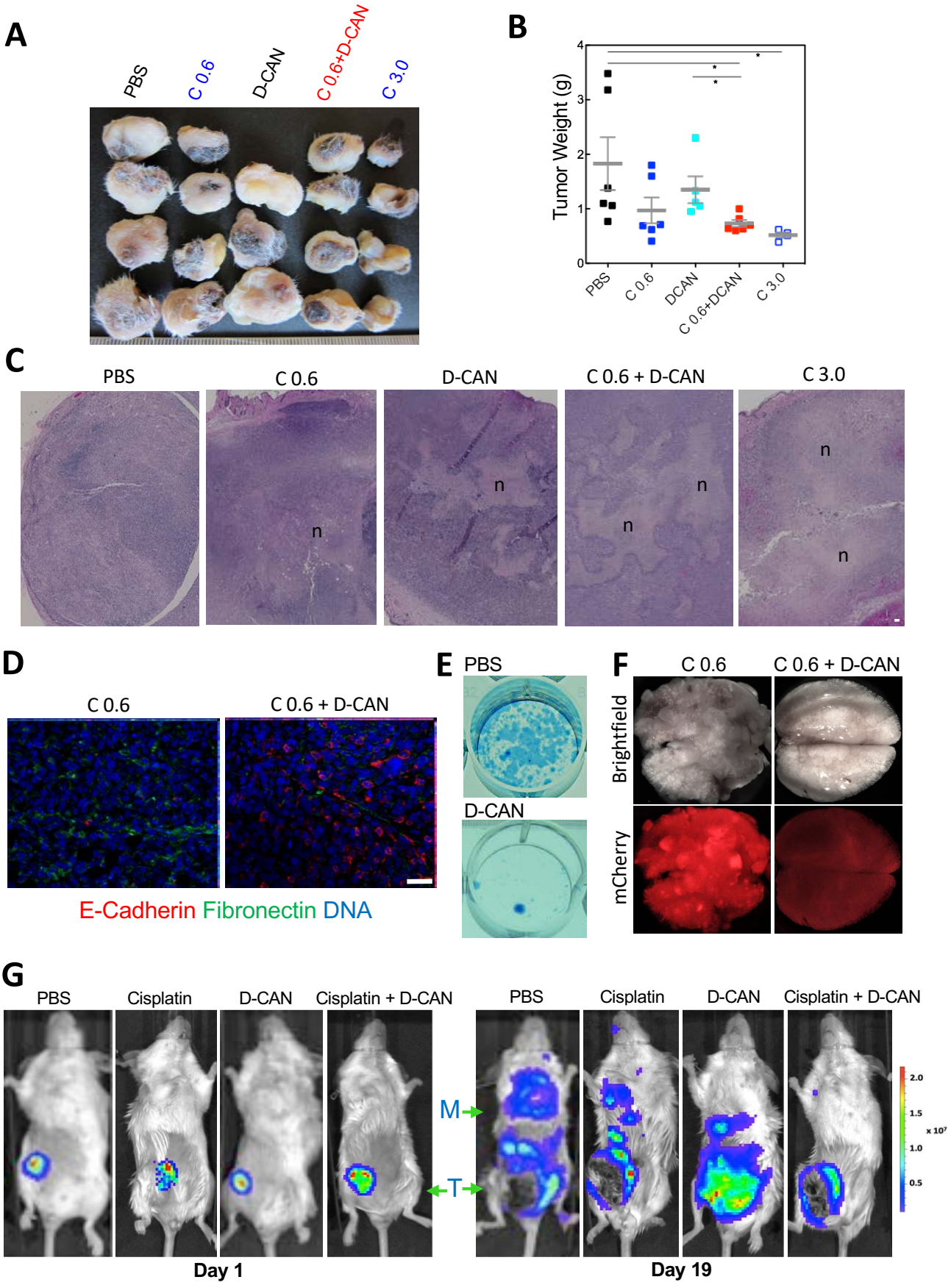

Supplementary Figure S2